Nanoscale Res Lett (2010) 5:237–242
DOI 10.1007/s11671-009-9471-y

NANO EXPRESS

Electrical Conductivity Studies on Individual Conjugated Polymer Nanowires: Two-Probe and Four-Probe Results

Yun Ze Long · Jean Luc Duvail · Meng Meng Li · Changzhi Gu · Zongwen Liu · Simon P. Ringer

Received: 20 August 2009 / Accepted: 14 October 2009 / Published online: 13 November 2009

Abstract Two- and four-probe electrical measurements on individual conjugated polymer nanowires with different diameters ranging from 20 to 190 nm have been performed to study their conductivity and nanocontact resistance. The two-probe results reveal that all the measured polymer nanowires with different diameters are semiconducting. However, the four-probe results show that the measured polymer nanowires with diameters of 190, 95–100, 35–40 and 20–25 nm are lying in the insulating, critical, metallic and insulting regimes of metal–insulator transition, respectively. The 35–40 nm nanowire displays a metal–insulator transition at around 35 K. In addition, it was found that the nanocontact resistance is in the magnitude of 10^4 Ω at room temperature, which is comparable to the intrinsic resistance of the nanowires. These results demonstrate that four-probe electrical measurement is necessary to explore the intrinsic electronic transport properties of isolated nanowires, especially in the case of metallic nanowires, because the metallic nature of the measured nanowires may be coved by the nanocontact resistance that cannot be excluded by a two-probe technique.

Keywords Nanowires · Conductivity · Nanocontact resistance · Conducting polymers · Template synthesis

Y. Z. Long (✉) · M. M. Li
College of Physics Science, Qingdao University, 266071 Qingdao, China
e-mail: yunze.long@163.com

J. L. Duvail
Institut des Matériaux Jean Rouxel, CNRS, Université de Nantes, 44322 Nantes, France

C. Gu
Beijing National Laboratory for Condensed Matter Physics, Institute of Physics, Chinese Academy of Sciences, 100190 Beijing, China

Z. Liu · S. P. Ringer
Australian Key Centre for Microscopy and Microanalysis, The University of Sydney, Sydney, NSW 2006, Australia

Introduction

Recently, one-dimensional nanostructures, such as carbon nanotubes [1], inorganic semiconductor nanowires [2] and conjugated polymer nanowires [3], have become the subject of intense investigations due to their importance for both fundamental research and potential applications in nanoscale devices. Among numerous kinds of nanostructures, conducting polymer nanowires and nanotubes, such as polyaniline, polypyrrole and poly(3,4-ethylenedioxythiophene) (PEDOT), are promising materials for fabricating polymeric nanodevices. By now, electronic transport properties (e.g., electrical conductivity) of nanodevices based on individual conducting polymer nanotubes and nanowires have been explored by various techniques such as the two-probe technique based on a conductive scanning probe microscope [4–6]. The common approach to the two-probe technique is generally realized by dispersing nanotubes/wires on photo- or electron-beam lithographic-prepatterned microleads or nanoleads and the subsequent searching of nanofibers lying on two or four leads only [7–12]. In addition, electron- and/or focused ion beam assisted deposition technique has been employed to attach metal microleads on isolated nanotubes/wires [13–18]. A facile technique for fabrication and measurement of polymer nanowire arrays between electrodes in channels was also reported [19].

Although lots of effort on the electronic transport measurement of individual polymer fibers has been done, some key questions are still unclear, such as whether the two-probe measurements can reveal the intrinsic electronic transport properties of single polymer nanowires and how the nanocontacts can affect the results. These questions are very important for the fabrication and characterization of nanodevices based on individual nanofibers through electron-beam lithography and/or focused ion beam deposition. Since an insulating or semiconducting layer could be formed at the interface between a metal lead and a nanowire/tube, the contact resistance of such electronic contact may be strongly temperature dependent and this can seriously complicate or even dominate the measured resistance of the nanowire/tube. Up to now, there have been efforts addressing this problem in the measurements of carbon nanotubes [20, 21] and individual metal oxide nanowires such as IrO_2 [22], SnO_2 [23], ZnO [24] and RuO_2 [25] nanowires. For instance, two- and four-probe electrical measurements on individual SnO_2 nanowires have been performed to evaluate their conductivity and contact resistance [23]. Lin et al. [24] have studied the electronic transport properties of a single ZnO nanowire and RuO_2 nanowire [25] through their contacts with a metal electrode. However, the nanocontact between a metal lead and a polymer nanowire has not been precisely explored yet.

In our previous works [15–18], we measured the electrical conductivity of isolated conjugated polymer nanofibers and the contact resistance of two crossed polyaniline nanotubes. In this paper, we focus on two- and four-probe electrical measurements on individual PEDOT nanowires with different diameters ranging from 20 to 190 nm. It was found that if the temperature dependence of the nanowire resistance is weak, the resistance of the nanocontact between a metal lead and a polymer nanowire can dominate the low-temperature resistance, and thus overshadow the metallic behavior of the measured nanowire. One such case is when the nanowire is lying in the metallic regime of metal–insulator transition. So a four-probe electrical measurement is necessary to reveal the intrinsic electronic transport properties of individual (metallic) polymer nanofibers.

Experimental

The PEDOT nanowires were prepared in templates of polycarbonate track-etched membranes [18, 26–28]. In a typical synthesis procedure, we used a gold layer evaporated on one side of the membrane as the working electrode, a platinum plate as the counter electrode and a saturated calomel electrode as the reference. The polymerization bath consisted of an aqueous solution containing 0.07 M sodium dodecyl sulfate, 0.1 M $LiClO_4$ and 0.05 M 3,4-ethylenedioxythiophene (provided by BAYER AG and distilled before using). The electrochemical polymerization was carried out at a fixed potential of 0.8 V vs. saturated calomel electrode with an EGG 273 potentiostat. After the polymerization, polycarbonate (the membrane template) was removed by dissolution with a flow of dichloromethane, and the nanowires were dispersed onto a SiO_2 wafer. The resulting PEDOT nanowires were characterized by a field-emission scanning electron microscope (SEM), a transmission electron microscope, Raman spectra, X-ray photoelectron spectra and electron spin resonance. More details can be found in Ref. [26–28].

The way of attaching Pt microleads on an isolated nanowire was described in previous publications [15–18]. First, we used a scanning electron microscope to find an appropriately isolated PEDOT nanowire on the wafer. Then, two pairs of Pt microleads typically 0.5 μm in width and 0.4 μm in thickness were fabricated by FIB deposition (Dual-Beam 235 FIB System from FEI Company, working voltage of the system is 5 kV for the electron beam and 30 kV for the focused ion beam, respectively, current of the focused ion beam is 1–10 pA), as shown in Fig. 1. Finally, electrical connection between the Pt microleads and the sample holder was made by highly conductive silver paste and gold wires. Electrical measurements of individual PEDOT nanowires were carried out using a Keithley 236 source measure unit in a helium gas flow cryostat (Oxford), or a Physical Property Measurement System from Quantum Design and a Keithley 6487 picoammeter/voltage source covering a wide temperature range of 10–300 K. The four-probe resistance was measured by applying a very small current ($I = 0.01$–10 nA, corresponding voltage $V =$ 0.0005–0.02 V) in a range where the I–V characteristics were linear. The two-probe resistance was determined under $V_{bias} = 0.02$ V. The same PEDOT nanowire was used for four-probe measurement first and then for two-probe measurement. The resistance of the polymer nanowire with a given diameter was measured at least twice, for example, under cooling and during heating. The reproducibility of the results has been good. In addition, for nanowires with a given diameter, two or more individual nanowires were measured to check the reproducibility.

Results and Discussion

As we know, in the four-probe method, the measured resistance R_{4P} is the intrinsic nanowire resistance of the measured segment. However, in the two-probe method, the measured resistance R_{2P} is given by $R_{2P} = R_{lead1} + R_{con1} + R_{4P} + R_{con2} + R_{lead2} = R_{lead} + R_{con} + R_{4P}$, where $R_{lead} = R_{lead1} + R_{lead2}$ is the resistance of the two microleads and $R_{con} = R_{con1} + R_{con2}$ is the contact resistance of

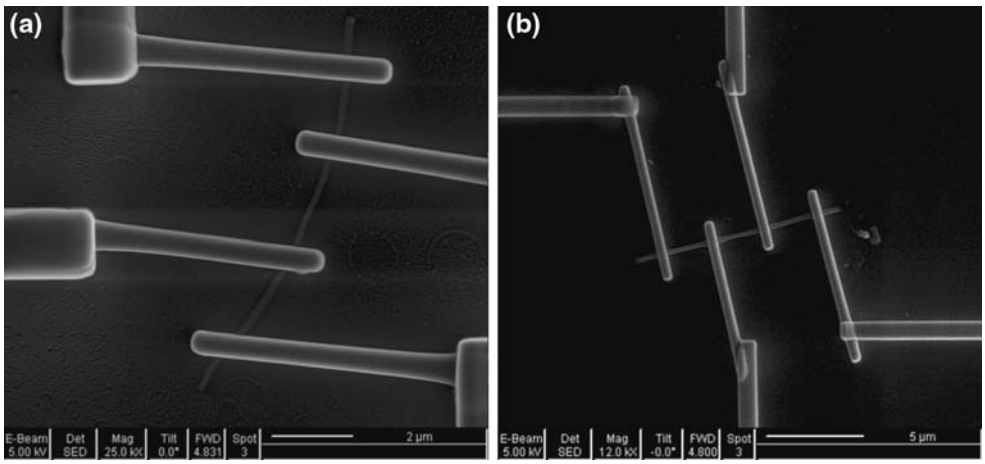

Fig. 1 SEM images of template-synthesized PEDOT nanowires and the attached four Pt microleads

the two microlead–nanowire contacts. The two major factors that affect the contact resistance are the geometry and the insulating layers (potential barriers) between the contacting surfaces. The resistance of a contact is inversely proportional to its area, and it is dependent on the force holding the two surfaces together, their stiffness and the respective electronic structure of the two materials. In the present case, the platinum microlead fabricated by FIB deposition can promise a good contact with the nanowire. However, insulating layers (potential barriers) between the nanowire and the platinum microleads are inevitable because they have different energy levels or work functions. In addition, contamination of the nanowire surfaces from solvent or water adsorption may also increase the potential barrier width and height.

In this study, the resistance R_{lead} of the two Pt microleads is less than 1 kΩ (estimated using the widely recognized resistivity of 5×10^{-4} Ω cm for the deposited Pt film under the conditions used for the FIB deposition [29]), whereas the nanowire resistance R_{4P} and the contact resistance R_{con} are usually larger than 20 kΩ (as described below). So, R_{lead} is negligibly small compared with R_{4P} and R_{con}, and hence can be ignored, thus we get $R_{2P} = R_{\text{con}} + R_{4P}$. It is obvious that if $R_{\text{con}} \gg R_{4P}$, then $R_{2P} \approx R_{\text{con}}$, and if $R_{\text{con}} \ll R_{4P}$, then it is $R_{2P} \approx R_{4P}$.

Through electrical measurements on many isolated PEDOT nanowires with different diameters, the room temperature conductivities of the nanowires with diameters of 190, 95–100, 35–40 and 20–25 nm were obtained that are about 11.2, 30–50, 490–530 and 390–450 S/cm, respectively. The room temperature conductivity increases with the decrease of outer diameter of the conducting polymer nanofibers. This was also reported by Martin et al. [30] previously, and could be ascribed to the enhancement of molecular and super-molecular ordering (alignment of the polymer chains).

Figure 2 shows the four-probe and two-probe test results of resistances for isolated PEDOT nanowires with different diameters ranging from 20 to 190 nm. For the 190 nm PEDOT nanowire that is lying in the insulating regime of the metal–insulator transition, as shown in Fig. 2a, the two-probe resistance R_{2P} is quite close to the four-probe resistance R_{4P} from 20 to 300 K, and both R_{2P} and R_{4P} have strong temperature dependence. These results indicate that compared with the intrinsic nanowire resistance of the measured segment, the microlead–nanowire contact resistance is small and negligible. For four-probe resistance of the 95–100 nm PEDOT nanowire, as shown in Fig. 2b, it has a relatively weak temperature dependence and is close to the critical regime of metal–insulator transition. It is interesting to find that the two-probe resistance R_{2P} is quite close to the four-probe resistance R_{4P} at higher temperature; however, at low temperature, R_{2P} increases sharply especially below 25 K and becomes much larger than R_{4P}. For the 35–40 nm PEDOT nanowire, as shown in Fig. 2c, the result of the four-probe resistance $R_{4P}(T)$ indicates that the nanowire is lying in the metallic regime of metal–insulator transition and there is a transition at around 35 K. It should be mentioned here that $R_{4P\text{-}1}(T)$ was measured first, and $R_{4P\text{-}2}(T)$ was measured 6 months later. However, the two-probe resistance R_{2P} only increases monotonously with temperature lowering, indicating that R_{2P} is dominated by the contact resistance that is $R_{2P} \approx R_{\text{con}}$, especially below 100 K. For the 20–25 nm PEDOT nanowire, which is also lying in an insulating regime, as shown in Fig. 2d, both R_{2P} and R_{4P} have strong temperature dependence. It seems that both R_{con} and R_{4P} are very large and cannot be ignored for the measured 20–25 nm nanowire.

Here, it should be noted that although the 20–25 nm PEDOT nanowire has a relatively high conductivity at room temperature (390–450 cm/S), the nanowire shows very strong temperature dependence (R(10 K)/R(300 K) ~ 10^5)

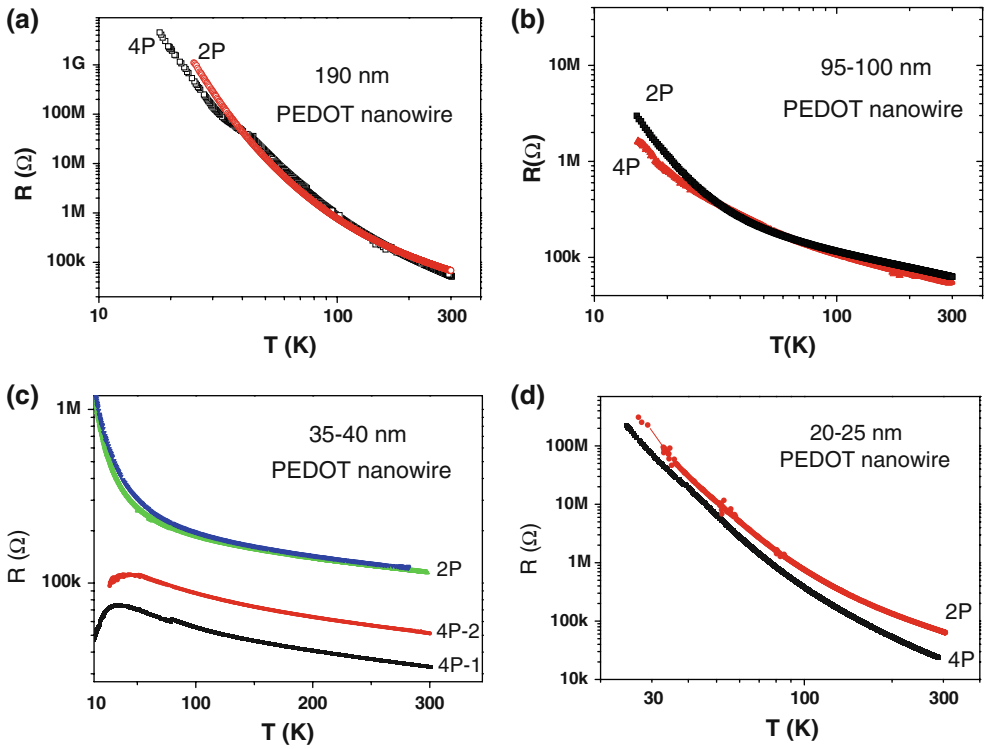

Fig. 2 Temperature dependence of four-probe (4P) and two-probe (2P) resistances for individual template-synthesized PEDOT nanowires with diameters **a** 190 nm, **b** 95–100 nm, **c** 35–40 nm and **d** 20–25 nm

or insulating behavior possibly due to confining effect limited by the small diameter of the nanowire. It is well known that such an effect should occur when a characteristic physical length is comparable to the diameter. In the present case, the diameter (20–25 nm) of the PEDOT nanowire is equal or close to the localization length of electrons *Lc* (*Lc* ∼ 20 nm for conducting polymers close to the metal–insulator transition [31]); therefore, localization of electrons induced by Coulomb interaction or small disorder must be taken into account in order to explain the insulating behavior especially at low temperature.

By employing the two-probe and four-probe methods, the electronic contact resistances, $R_{con}(T)$, have been determined. We found that the room temperature R_{con} and R_{4P} for the PEDOT nanowires are at the same order of magnitude. For example, R_{con} is 63 and 46 kΩ, and R_{4P} is 53 and 24 kΩ for the measured 35–40 and 20–25 nm PEDOT nanowires, respectively. However, $R_{con}(T)$ increases rapidly with decreasing temperature, as shown in Fig. 3, indicating an insulating or semiconducting contact formed at the interfaces between the Pt microlead and the polymer nanowire. Lin et al. [25] reported the electronic contact resistances formed between electron-beam lithographic-patterned submicron Cr/Au electrodes and single metallic RuO_2, IrO_2 and Sn-doped In_2O_{3-x} nanowires. They found that the contact resistances can range from several tens/hundreds of Ohm to several tens of kOhm at 300 K, and their temperature dependences can be well described by a thermal fluctuation-induced tunneling (FIT) conduction model proposed by Sheng [32], which describes the temperature-dependent resistance across a single small junction as $R(T) = R_0\exp[T_1/(T_0 + T)]$, where R_0 is a parameter that weakly depends on temperature only, and T_1 and T_0 are characteristic temperatures. In the present case, the fitting values for the three parameters R_0, T_1 and T_0 are 52 kΩ, 63.6 K and 5.16 K for the 35–40 nm nanowire, and

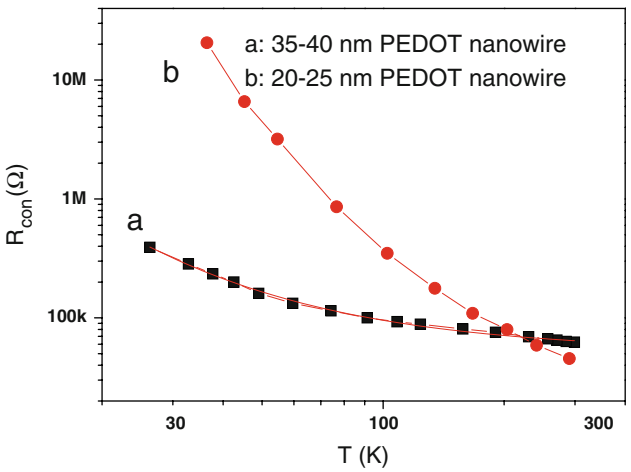

Fig. 3 Temperature dependence of nanocontact resistance ($R_{con} = R_{2P} - R_{4P}$) determined from Fig. 2c, d

37 kΩ, 255.2 K and 4.04 K for the 20–25 nm PEDOT nanowire, respectively. Here, for comparison, the contact resistances of the 190 and 95–100 nm nanowires have been the calculated contact resistances that are equal to 11 and 18 KΩ at room temperature, respectively, and are smaller than that in the case of 35–40 and 20–25 nm nanowires (63 and 46 kΩ). It seems that owing to the decrease of the contact area between the nanowire and the platinum microleads, the nanocontact resistance at low temperature increases with diameter decreasing and shows much stronger temperature dependence.

The earlier results demonstrate that the nanocontact resistance is an important issue in electrical resistance measurements on isolated nanowires, which may dominate the measured two-probe resistance especially at low temperatures. Compared with the two-probe method, we believe that the four-probe measurement can further reveal the intrinsic electronic transport properties of the nanowires. For example, the two-probe results in Fig. 2 just indicate that all the measured PEDOT nanowires are semiconducting. However, the four-probe results reveal the metallic behavior of the 35–40 nm PEDOT nanowire below 35 K. In addition, for individual RuO_2 nanowires [25], it was also reported that the temperature dependence of two-probe resistance indicates that the nanowire is semiconducting, whereas the four-probe resistance dependence of the same nanowire shows the measured nanowire is metallic.

Though the metallic behavior and metal–insulator transition have been observed in bulk films of doped polyacetylene, polypyrrole, PEDOT, poly(*p*-phenylenevinylene) (PPV) and polyaniline [31, 33–35], similar metallic behavior and metal–insulator transition have rarely been reported for isolated polymer nanowires/tubes. It is generally believed that nanosize effect, disorder-induced localization of the charge carriers and enhanced electron–electron interaction-induced localization could be possible reasons to degrade the metallic behavior of nanowires/tubes [3, 9, 15, 18, 36]. Based on our results, we propose that nanocontact resistance may be one of the key reasons for this degradation. In most published results, the temperature-dependent resistance of a single nanowire/tube was determined by two-probe technique; therefore, the metallic nature of the measured polymer fibers could be overshadowed by the nanocontact resistance especially at low temperatures (such as the 35–40 nm PEDOT nanowire as shown in Fig. 2c) although the nanofibers show a relatively high electrical conductivity at room temperature.

Conclusions

In summary, we have performed two- and four-probe electrical measurements on individual conducting polymer PEDOT nanowires with different diameters ranging from 20 to 190 nm. The four-probe results reveal that the measured PEDOT nanowires with diameters of 190, 95–100, 35–40 and 20–25 nm are lying in the insulating, critical, metallic and insulting regimes of metal–insulator transition, respectively. The two-probe results, however, reveal that all the measured PEDOT nanowires are semiconducting due to the microlead–nanowire contact resistances that show semiconducting or insulating behavior at low temperatures. These results indicate that four-probe electrical measurement is necessary to explore the intrinsic electronic transport properties of individual nanowires, especially in the case of metallic nanowires due to the effect of the nanocontact resistance that cannot be excluded in the two-probe measurement.

Acknowledgments This work was financially supported by the National Natural Science Foundation of China (Grant No 10604038) and the Program for New Century Excellent Talents in University of China (Grant No NCET-07-0472) and by the Communauté urbaine de Nantes, France.

References

1. P. Sharma, P. Ahuja, Mater. Res. Bull. **43**, 2517 (2008)
2. Y. Xia, P. Yang, Y. Sun, Y. Wu, B. Mayers, B. Gates, Y. Yin, F. Kim, H. Yan, Adv. Mater. **15**, 353 (2003)
3. A.N. Aleshin, Adv. Mater. **18**, 17 (2006)
4. J.G. Park, S.H. Lee, B. Kim, Y.W. Park, Appl. Phys. Lett. **81**, 4625 (2002)
5. S.K. Saha, Y.K. Su, C.L. Lin, D.W. Jaw, Nanotechnology **15**, 66 (2004)
6. L. Liu, Y. Zhao, N. Jia, Q. Zhou, C. Zhao, M. Yan, Z. Jiang, Thin Solid Films **503**, 241 (2006)
7. A.G. MacDiarmid, W.E. Jones, I.D. Norris, J. Gao, A.T. Johnson, N.J. Pinto, J. Hone, B. Han, F.K. Ko, H. Okuzaki, M. Llaguno, Synth. Metals **119**, 27 (2001)
8. J.G. Park, G.T. Kim, V. Krstic, B. Kim, S.H. Lee, S. Roth, M. Burghard, Y.W. Park, Synth. Metals **119**, 53 (2001)
9. S. Samitsu, T. Shimonura, K. Ito, M. Fujimori, S. Heike, T. Hashizume, Appl. Phys. Lett. **86**, 233103 (2005)
10. B.K. Kim, Y.H. Kim, K. Won, H. Chang, Y. Choi, K.J. Kong, B.W. Rhyu, J.J. Kim, J.O. Lee, Nanotechnology **16**, 1177 (2005)
11. B.H. Kim, D.H. Park, J. Joo, S.G. Yu, S.H. Lee, Synth. Metals **150**, 279 (2005)
12. L. Gence, S. Faniel, C. Gustin, S. Melinte, V. Bayot, V. Callegari, O. Reynes, S. Demoustier-Champagne, Phys. Rev. B **76**, 115415 (2007)
13. X. Zhang, J.S. Lee, G.S. Lee, D.K. Cha, M.J. Kim, D.J. Yang, S.K. Manohar, Macromolecules **39**, 470 (2006)
14. Z.H. Yin, Y.Z. Long, C.Z. Gu, M.X. Wan, J.L. Duvail, Nanoscale Res. Lett. **4**, 63 (2009)
15. Y.Z. Long, L.J. Zhang, Z.J. Chen, K. Huang, Y.S. Yang, H.M. Xiao, M.X. Wan, A.Z. Jin, C.Z. Gu, Phys. Rev. B **71**, 165412 (2005)
16. Y.Z. Long, Z.J. Chen, J.Y. Shen, Z. Zhang, L.J. Zhang, K. Huang, M.X. Wan, A. Jin, C.Z. Gu, J.L. Duvail, Nanotechnology **17**, 5903 (2006)
17. Y.Z. Long, L.J. Zhang, Y.J. Ma, Z.J. Chen, N.L. Wang, Z. Zhang, M.X. Wan, Macromol. Rapid Commun. **24**, 938 (2003)

18. Y.Z. Long, J.L. Duvail, Z.J. Chen, A.Z. Jin, C.Z. Gu, Chin. Phys. Lett. **25**, 3474 (2008)
19. K. Ramanathan, M.A. Bangar, M. Yun, W. Chen, A. Mulchandani, N.V. Myung, Nano Lett. **4**, 1237 (2004)
20. C. Lan, P. Srisungsitthisunti, P.B. Amama, T.S. Fisher, X. Xu, R.G. Reifenberger, Nanotechnology **19**, 125703 (2008)
21. Q. Chen, S. Wang, L.M. Peng, Nanotechnology **17**, 1087 (2006)
22. Y.H. Lin, Y.C. Sun, W.B. Jian, H.M. Chang, Y.S. Huang, J.J. Lin, Nanotechnology **19**, 045711 (2008)
23. F. Hernández-Ramírez, A. Tarancón, O. Casals, J. Rodríguez, A. Romano-Rodríguez, J.R. Morante, S. Barth, S. Mathur, T.Y. Choi, D. Poulikakos, V. Callegari, P.M. Nellen, Nanotechnology **17**, 5577 (2006)
24. Y.F. Lin, W.B. Jian, C.P. Wang, Y.W. Suen, Z.Y. Wu, F.R. Chen, J.J. Kai, J.J. Lin, Appl. Phys. Lett. **90**, 223117 (2007)
25. Y.H. Lin, S.P. Chiu, J.J. Lin, Nanotechnology **19**, 365201 (2008)
26. J.L. Duvail, P. Rétho, V. Fernandez, G. Louarn, P. Molinié, O. Chauvet, J. Phys. Chem. B **108**, 18552 (2004)
27. J.L. Duvail, Y.Z. Long, S. Cuenot, Z. Chen, C. Gu, Appl. Phys. Lett. **90**, 102114 (2007)
28. J.L. Duvail, Y. Long, P. Retho, G. Louarn, L. Dauginet De Pra, S. Demoustier-Champagne, Mol. Cryst. Liq. Cryst. **485**, 835 (2008)
29. G.D. Marzi, D. Iacopino, A.J. Quinn, G. Redmond, J. Appl. Phys. **96**, 3458 (2004)
30. C.R. Martin, Acc. Chem. Res. **28**, 61 (1995)
31. R. Menon, C.O. Yoon, D. Moses, A.J. Heeger, in *Handbook of conducting polymers*, 2nd edn., ed. by T.A. Skotheim, R.L. Elsenbaumer, J.R. Reynolds (Marcel Dekker, New York, 1998), p. 85
32. P. Sheng, Phys. Rev. B **21**, 2180 (1980)
33. A.J. Heeger, Synth. Metals **125**, 23 (2002)
34. Y.Z. Long, Z.J. Chen, N.L. Wang, J.C. Li, M.X. Wan, Physica B **344**, 82 (2004)
35. K. Lee, S. Cho, S.H. Park, A.J. Heeger, C.W. Lee, S.H. Lee, Nature **441**, 65 (2006)
36. Y.B. Khavin, M.E. Gershenson, A.L. Bogdanov, Phys. Rev. B **58**, 8009 (1998)